Biointerface Research in Applied Chemistry
Open-Access Journal (ISSN: 2069-5837)

Article
Volume 13, Issue 4, 2023, 376
https://doi.org/10.33263/BRIAC134.376

Evaluation of Terpenoids as Dipeptidyl Peptidase 4 Lead Molecules: Molecular Docking and Dynamics Simulation Study

Iqra Khan [1], Mohammad Kalim Ahmad Khan [1,*], Salman Akhtar [1]

[1] Department of Bioengineering, Integral University, Lucknow, 226026, Uttar Pradesh, India; ikhan0100606@gmail.com (I.K.); mkakhan@iul.ac.in (M.K.A.K.); sakhtar@iul.ac.in (S.A.);
* Correspondence: mkakhan@iul.ac.in (M.K.A.K.);

Scopus Author ID 57193235237
Received: 19.08.2022; Accepted: 19.09.2022; Published: 31.10.2022

Abstract: About 966 billion US dollars have been spent globally treating and managing diabetic patients. Notwithstanding individuals' substantial access to the required primary medical services and essential medicines, it is tempting to get momentum in identifying new chemical entities, biologics, or small molecules as drug candidates that are prophylactically and therapeutically effective against lifestyle-based maladies, thereby backing the overall health mission of Sustainable Development Goals. Towards this context, the study aims to screen natural inhibitor(s) targeting dipeptidyl peptidase 4 using hybrid approaches of bioinformatics and medicinal chemistry. Data set of 513 ligands of terpenoids in nature was retrieved from the naturally occurring plant-based anticancerous compound-activity-target database (NPACT) and performed docking studies. Sitagliptin depicted substantial binding affinity among reference drugs with dipeptidyl peptidase 4 (DPP IV) (binding energy: -8.63 kcal/mol, Inhibition constant: 163.65 μM). Among all terpenoids, Asiatic acid (ΔG: -9.95 kcal/mol, 85.23 μM), Aucubin (-9.86 kcal/mol, 98.98 μM), Ailanquassin A (-9.25 kcal/mol, 156.23 μM), and 6-α-hydroxyneopulchellin (-9.18 kcal/mol, 189.76 μM) depicted strong binding affinities with DPP IV compared to Sitagliptin. Based on the MD simulation findings, Asiatic acid and Aucubin were better lead molecules than Sitagliptin. However, holistic wet-lab validations are required before manifesting their therapeutic implications against diabetes.

Keywords: diabetes; DPP IV; docking; molecular dynamics; Sitagliptin; Asiatic acid

1. Introduction

Diabetes mellitus chronically increases blood glucose levels due to absolute or relative insulin deficiency. It is highly prevalent, and its complications are among the leading causes of death. As per the statistics of the International Diabetes Federation (IDF) diabetes atlas edition 10.0, 2021, more than 537 million individuals aged 20-79 years were diagnosed with diabetes that may be worst and may uprise to 643 million, bypassing 2030, and 783 by 2045, in which 6.7 million individuals demises could be documented globally, especially in those countries that are socially and economically underprivileged [1,2]. Almost 966 billion US dollars, a tremendous amount of money, have been allotted to treating and managing this lifestyle-based disease. Diabetes is considered socially significant morbidity because of its considerable negative impact on the patients' duration and quality of life. Therefore, research activities focus on developing novel, more effective therapies to improve glucose homeostasis and alleviate

insulin resistance. According to its pathogenesis, two main types of diabetes can be distinguished – diabetes mellitus type 1 (T1DM) and type 2 (T2DM). However, novel diabetic subgroups based on additional factors for the disease's occurrence, such as body-mass index, age, β-cell function, insulin resistance, and presence of autoantibodies, aim at a more precise and individualized therapeutic handling. Type 1 diabetes mellitus (T1DM) typically has a sudden onset caused by a pancreas dysfunction resulting in insufficient or completely abolished insulin production and secretion. Common symptoms are frequent urination (polyuria), excessive thirstiness (polydipsia), hunger (polyphagia), fatigue, blurry vision, unexpected weight loss, and delayed wound healing. This category of diabetes is caused by autoimmune processes targeting insulin-producing β-cells. It usually occurs at a young age. However, a form of T1DM manifesting later in adulthood also exists called latent autoimmune diabetes of adults (LADA). It can be falsely diagnosed as T2DM [3,4].

The risk of short- and long-term complications necessitates tight blood glucose control. Novel medical devices that have recently been approved or are undergoing clinical trials may improve diabetics' quality of life. Such devices are insulin pumps, closed-loop glucose monitoring systems, and artificial bionic pancreas. T1DM is managed by insulin replacement treatment. With type 2 diabetes, our body does not use insulin well and cannot manage optimum blood sugars. More than 90% of individuals with T2DM took a long time to develop and diagnose. We may not notice any symptoms, so we must get our blood sugar tested if we are at risk. T2DM can be prevented or delayed with healthy lifestyle changes, such as losing weight, eating healthy food, being active, and taking proper medications [5-9]. According to the International Diabetes Federation (IDF), in 2019, diabetes occurrence and projections by 2030 and 2030 have been shown in Figure 1 [10,11].

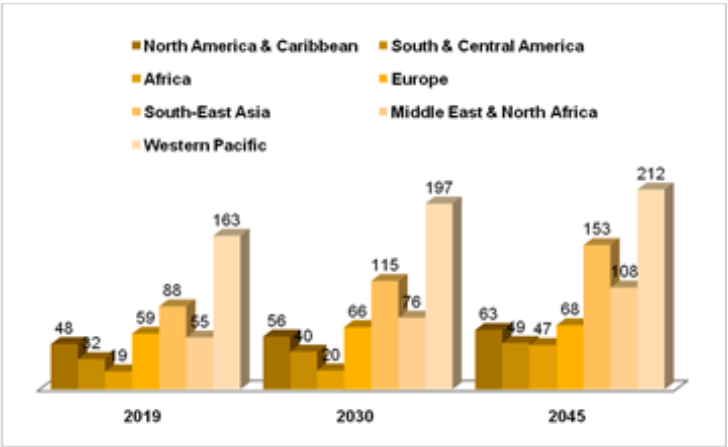

Figure 1. Comparative statistics of diabetic patients in 2019, 2030, and 2045 aged between 20-79 years. The number of occurrences and projections are exhibited in millions.

Besides the ample amount of therapeutic and prophylactic drugs, it is difficult to control diabetes in totality. From the very beginning, pharmaceutical industries have been shifting their attention toward identifying therapeutically potential molecular targets using various interdisciplinary approaches of genomics, proteomics, system biology, traditional experimental biology, and biomedical sciences. Despite having various robust and sophisticated high-throughput technologies, the process of finding new drug candidates and their development as therapeutics is moving at a slow pace, viz., identification of small molecules as new lead molecules from millions of investigational ligands takes about ten years and about $2-3 billion, including from SBVS, preclinical and clinical experiments, regulatory approval, and launch to

the market. Molecular modeling, SBDD, LBDD, and machine learning approaches can accelerate the process, minimize attrition, and depict the ADMET and medicinal chemistry features, curtailing research and development costs and time [12].

DPP IV (dipeptidyl peptidase 4) was chosen as an essential protein target for identifying terpenoids as plausible inhibitors. DPP IV deactivates a group of metabolic hormones of the gastrointestinal tract, also known as incretins, that facilitate insulin release at physiological pH. The gastric inhibitory peptides GIP (gluco-dependent insulinotropic polypeptide) and GLP-1 (glucagon-like peptide-1) are induced after food. The α-cells and induced β-cells of pancreatic islets of Langerhans are deactivated by both GIP and GLP-1, thereby lowering the blood glucose level [13-16]. DPP IV is a GIP and GLP-1 antagonist, inducing glucagon release and inhibiting insulin secretion, thus facilitating hyperglycemia. Most DPP IV drugs, e.g., Gliptins family and peptide mimetics, inhibit DPP IV and induce incretins ensuing homeostasis of glucose level [17-19].

The study aims to identify the most probable lead molecules against diabetes via molecular interactions of DPP IV with 513 terpenoids using ADT (AutoDock Tools) [20]. Comparison of the docking and MD simulation findings with reference drug Sitagliptin favor the substantial and stable molecular interactions of Asiatic acid and Aucubin within the critical residues of the target protein.

2. Materials and Methods

2.1. Protein retrieval and optimization.

The PDB (3WQH) structure of the human DPP IV co-crystallized with the anagliptin was retrieved from the RCSB protein data bank. The only apoprotein was considered for preparing an input PDB file suitable for molecular docking via cleaning undesired atoms, ions, and molecules viz., NAG), SKK, inhibitor anagliptin, and H2O molecules. The 3D coordinates of anagliptin binding pockets were taken forward for docking interactions of terpenoids. The molecular mechanic's force field, CHARMm, was assigned to energetically optimize ligands'3D structure using a SMART algorithm to eliminate the steric hindrances and clashes [21-24].

2.2. Ligands retrieval and optimization.

The standard data format (SDF) of all terpenoids (513 molecules) was retrieved from the National Center for Biotechnology Information (NCBI) PubChem database. Likewise, 2D structures of known drug molecules in SDF format were also extracted. 2D SDF to 3D PDB conversion was accomplished through Accelrys discovery studio visualizer (DSV). All ligand molecules were energetically minimized and optimized through the same protocol as the target protein.

2.3. Docking simulation.

Molecular docking of terpenoids and reference drug Sitagliptin with DPP IV was carried out with ADT to get the most probable pattern of their binding strength. Four input files were prepared to run the ADT, viz., PDBQTs of both ligand and protein, GPF, and DPF. The grid box around the protein molecule was drawn with variable grid points in the x, y, and z axes and maximum spacing (1.00 Å) between two consecutive grids. Ten runs for each ligand

took into account. Minimum free energy of binding (ΔG) and inhibition constant (Ki) was chosen as selective filters for determining the most stable conformations docked into the binding pocket of the target protein [25-29].

2.4. ADMET profiling.

The terpenoids exhibiting ΔG lesser than the reference drug Sitagliptin were evaluated on different ADMET descriptors, physicochemical properties, lipophilicity, solubility, pharmacokinetics, drug-likeness, and medicinal chemistry attributes through the SwissADME [30].

2.5. Molecular dynamics simulation.

The molecular dynamics (MD) simulation study of the best-docked complex of terpenoid and DPP IV, along with a docked complex of Sitagliptin and DPP IV, was carried out using the online digital platform iMODS, a robust and fast computational tool for calculating the flexibility and stability of target protein upon binding with ligands [31]. An illustration of the adopted methodology of the proposed study is shown in Figure 2.

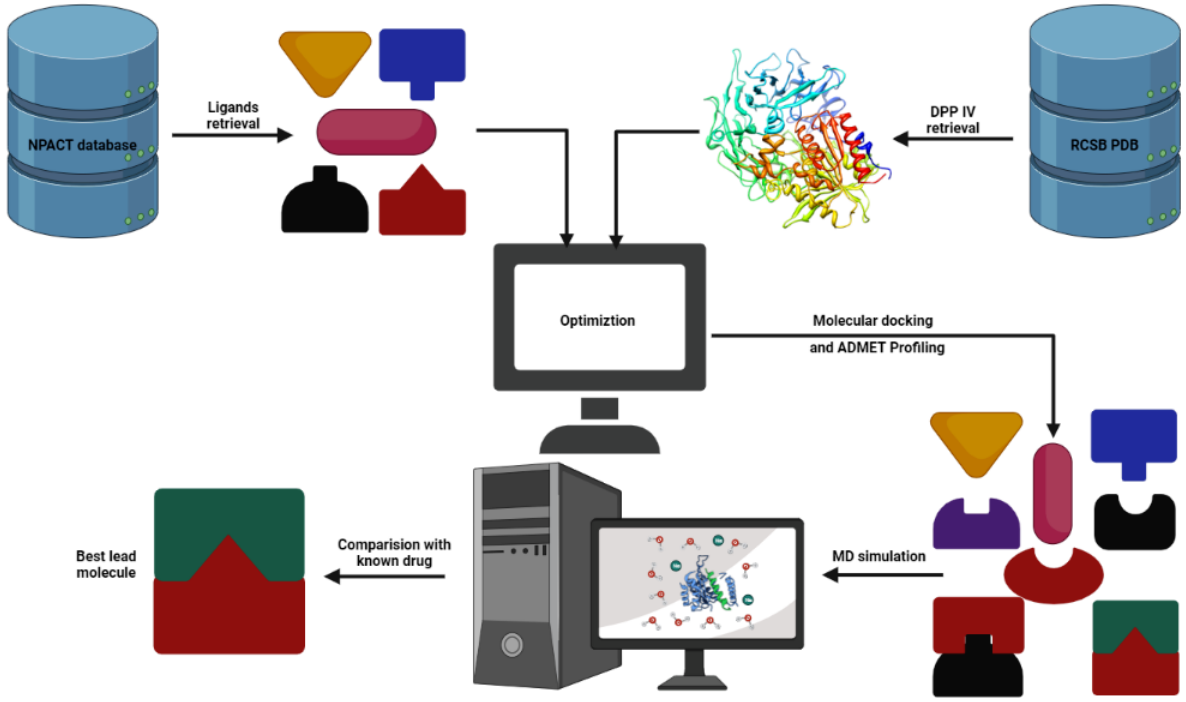

Figure 2. Flowchart of adopted methodology for identifying the potential lead molecules affecting DPP IV.

3. Results and Discussion

3.1. Molecular docking.

All terpenoids and reference drug Sitagliptin were docked to DPP IV to find one of the most plausible binding interactions of their respective confirmations. Terpenoids exhibit free energy of binding (ΔG) between -9.95 to -5.35 kcal/mol and inhibition constant (Ki) in the range of 85.23 μM to 687.20 μM. Sitagliptin, a reference molecule, depicts substantial binding affinity with DPP IV, having ΔG -8.63 kcal/mol and Ki 163.65 μM. Nine ligands out of 513 viz., Carnosol, Jatropholone, Rosmanol, Tagitinin, Ailanquassin, Bigelovin, Asiatic acid, Aucubin, and 6-α-hydroxyneopulchellin were showing better binding interactions as compared

to the Sitagliptin. Asiatic acid and Aucubin showed strong binding propensities toward DPP IV, as reflected by their ΔG (-9.95, -9.86 kcal/mol) and Ki (85.23, 98.98 μM) values, respectively. Moreover, Asiatic acid interacted with 14 residues of DPP IV through four different binding forces rendering stability to the complex viz., van der Waals, conventional H-bonds, pi-sigma, and pi-alkyl (Figure 3).

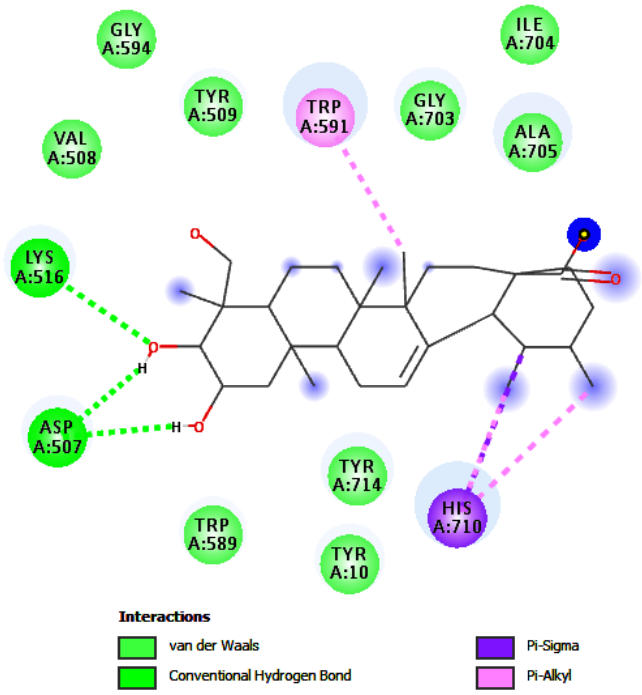

Figure 3. DPP IV-Asiatic acid complex. 2D diagram showing the DPP IV residues bind to Asiatic acid through van der Waals, hydrogen bond, pi-sigma, and pi-alkyl forces.

Likewise, Aucubin exhibited interaction with 12 residues of DPP IV through five different binding forces providing stability to the docked complex viz., van der Waals, conventional H-bonds, carbon-hydrogen bonds, alkyl, and pi-alkyl (Figure 4).

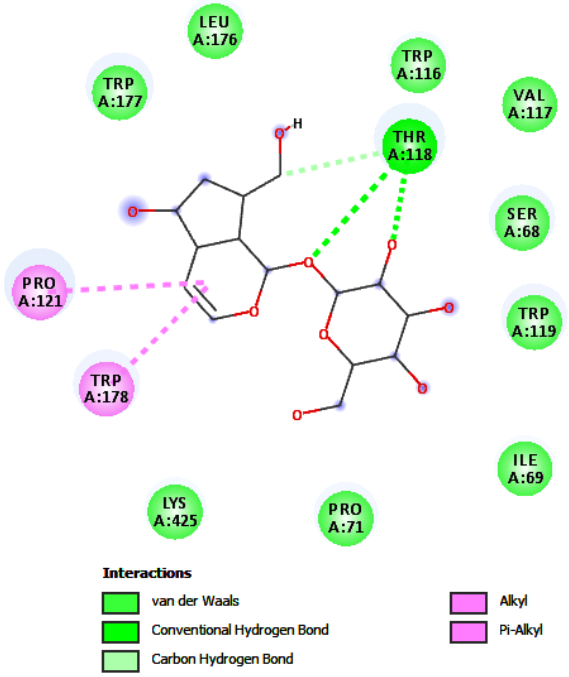

Figure 4. DPP IV-Aucubin complex. 2D diagram showing the DPP IV residues bind to Aucubin through van der Waals, hydrogen bond, carbon-hydrogen bond, alkyl, and pi-alkyl forces.

The reference drug Sitagliptin interacted with 13 residues of DPP IV via six different binding forces making the docked complex stable viz., van der Waals, conventional H-bonds, carbon-hydrogen bonds, halogen, pi-sigma, and pi-Sulphur (Figure 5).

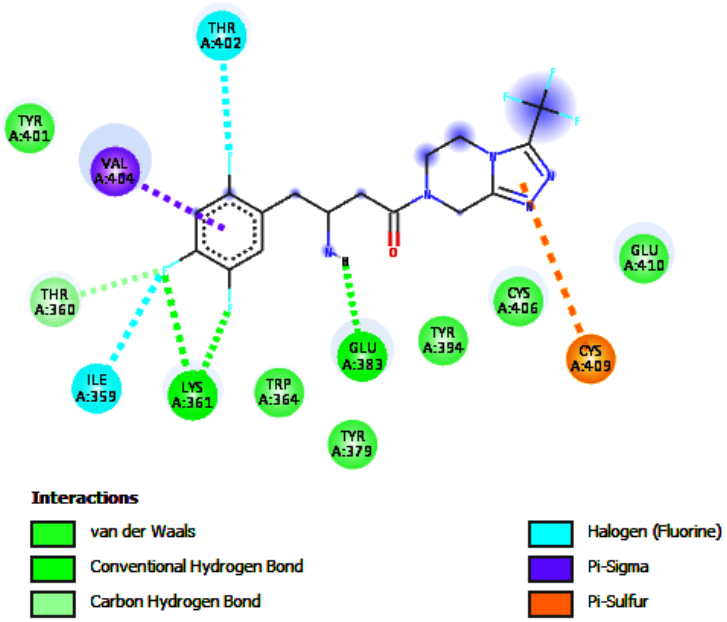

Figure 5. DPP IV-Sitagliptin complex. 2D diagram showing the DPP IV residues bind to Sitagliptin through van der Waals, hydrogen bond, carbon-hydrogen bond halogen, pi-sigma, and pi-sulfur forces.

3.2. ADMET assessment.

Egan-Egg or BOILED-Egg (Brain Or IntestinaL EstimateD) model was used to assess the ADMET features. This model forecasts edge values for two essential descriptors, e.g., human intestinal absorption (HIA) and blood-brain barrier (BBB) penetration. HIA and BBB rely on two crucial physiochemical properties, lipophilicity (reference WLOGP ≤ 5.88) and topological polar surface area (reference TPSA ≤ 131.6), and exhibits a clear graphical representation of the ligands threshold desired for HIA and BBB permeation [32-34]. As per its name, the Egan-Egg model has two regions, i.e., the yolk (yellow) and the white part, respectively, revealing intestinal absorption and brain penetration. Only nine terpenoids showing better affinities towards target protein DPP IV than Sitagliptin were passed through this model. Three ligands, namely Jatropholone, Carnosol, and Bigelovin, are located within the yolk region, which means they are good BBB penetrators and HIA permeator. Five ligands, Rosmanol, Tagitinin, Ailanquassin, Asiatic acid, and 6-alpha-hydroxyneopulchellin, are positioned in the white region of the egg, which means that they are showing good HIA absorption. Ligand Aucubin is positioned out of the white and yolk region, showing neither brain permeation nor intestinal absorption. Sitagliptin shows excellent BBB permeation and intestinal absorption (Figure 6). despite having substantial brain permeation, ligands Jatropholone and Carnosol effluxed out because of glycoprotein (P-gp) substrate. Likewise, the reference drug was also thrown out from the yolk region because of its propensity towards P-gp binding.

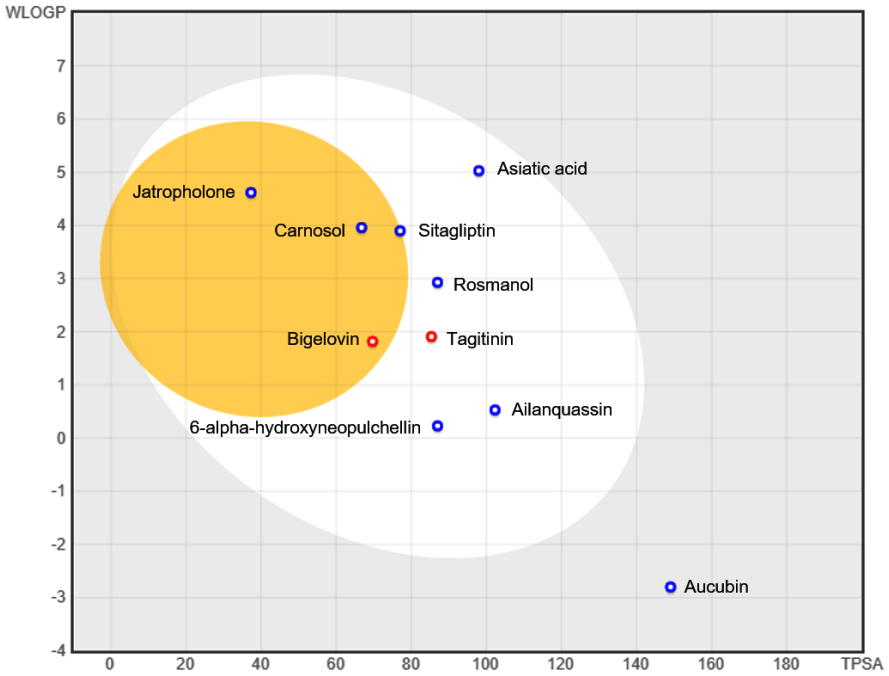

Figure 6. The Egan-Egg model for assessment of passive human intestinal absorption (HIA) and blood-brain barrier (BBB) penetration in the function of the position of selected terpenoids and reference drug. The blue and red dots represent P-gp positive and P-gp negative molecules, respectively.

3.2.1. Physicochemical properties.

Molecular weight (MW), the fraction of carbons in the sp3 hybridization (FCsp3), rotatable bond (RB), hydrogen bond acceptor (HBA), hydrogen bond donor (HBD), molar refractivity (MR), and polar surface area (PSA), key molecular and physicochemical descriptors play an essential role in the quick prediction of ADME attributes of small molecules. OpenBabel v2.3.0 was used to calculate the ADME descriptors. Moreover, SwissADME implies a fragmental technique to evaluate the PSA of chemical compounds, popularly known as topological polar surface area (TPSA) [35,36]. The computed physicochemical properties of selected ligands and Sitagliptin is shown in Table 1.

Table 1. Computed Physicochemical properties of selected terpenoids and reference molecules.

Ligands	MW	FCsp3	RB	HBA	HBD	MR	TPSA
Carnosol	330.42	0.65	1	4	2	92.83	66.76
Jatropholone	296.40	0.55	0	2	1	90.7	37.3
Rosmanol	346.42	0.65	1	5	3	93.99	86.99
Tagitinin	350.41	0.68	3	6	1	91.01	85.36
Ailanquassin	364.39	0.79	1	7	2	87.9	102.29
Bigelovin	304.34	0.59	2	5	0	79.05	69.67
Asiatic acid	488.70	0.90	2	5	4	139.24	97.99
Aucubin	346.33	0.73	4	9	6	77.15	149.07
6-alpha-hydroxyneopulchellin	282.33	0.80	0	5	3	71.91	86.99
Sitagliptin	407.31	0.44	6	10	1	87.25	77.04

Reference range: MW ≤ 500 g/m, HBA ≤ 10, HBD ≤ 5, $FCsp^3 \geq 0.25$, RB ≤ 10, 40 ≤ MR ≤ 130, TPSA≤ 150 $Å^2$

3.2.2. Lipophilicity.

Lipophilicity is an important physical property that governs solubility absorption, plasma protein binding, metabolic clearance, the volume of distribution, enzyme and receptor binding, biliary and renal clearance, brain penetration, and storage in tissues bioavailability, and toxicity. It can be defined as a partition coefficient between n-octanol and water. Mathematically, it can be expressed as:

$LogP_{o/w}$ = log (concentration of ligand in octanol/concentration of ligand in water)

The computed lipophilicity of the selected ligands and Sitagliptin is shown in Table 2.

Table 2. Computed lipophilicity of selected terpenoids and reference molecules.

Ligands	iLOGP	XLOGP3	WLOGP	MLOGP	SLogP	CLogP
Carnosol	2.97	4.38	3.96	3.25	4.05	3.72
Jatropholone	3.23	4.49	4.62	3.82	5.24	4.28
Rosmanol	2.5	3.41	2.93	2.42	3.16	2.88
Tagitinin	2.76	1.73	1.91	1.66	2.37	2.09
Ailanquassin	2.02	0.12	0.53	1.36	1.26	1.06
Bigelovin	2.13	1.19	1.82	1.92	2.08	1.83
Asiatic acid	3.2	5.7	5.03	4.14	3.96	4.41
Aucubin	1.44	-3.02	-2.8	-2.29	-2.78	-1.89
6-alpha-hydroxyneopulchellin	1.67	0.72	0.23	0.88	0.55	0.81
Sitagliptin	2.35	0.7	3.9	2.52	3.08	2.51

Reference range: XLogP3 (-2 to 5), WLogP (-0.4 to 5.88), MLogP (≤ 4.15)

3.2.3. Solubility.

Solubility determines intestinal absorption and oral bioavailability. The low solubility hinders absorption and causes low oral bioavailability. Molecular properties for solubility and permeability are opposed. Optimum solubility is required for intravenous formulation. SwissADME uses three descriptors adapted from the ESOL model, Ali *et al*., 2012 [37], and SILICOS-IT filter to predict the water solubility of small molecules at the log S scale, which is a decimal logarithm of the molar solubility in water. Optimum range for water solubility follows the order as insoluble <−10 < poorly <−6 < moderately <−4 < soluble <−2 < very < 0 < highly [37]. Table 3 shows the computed water solubilities of terpenoids and reference molecules, revealing that they either fall in the soluble, moderate soluble, or poorly soluble category.

Table 3. Computed solubility of selected terpenoids and reference molecules.

Ligands	Log *S* (ESOL)	Log *S* (Ali)	Log *S* (SILICOS-IT)
Carnosol	-4.77	-5.5	-4.45
Jatropholone	-4.71	-4.99	-5.42
Rosmanol	-4.25	-4.92	-3.64
Tagitinin	-2.9	-3.14	-2.22
Ailanquassin	-2.11	-1.82	-1.6
Bigelovin	-2.34	-2.25	-2.32
Asiatic acid	-6.33	-7.52	-4.28
Aucubin	0.18	0.45	2.76
6-alpha-hydroxyneopulchellin	-2.04	-2.13	-0.64
Sitagliptin	-2.7	-1.9	-4.81

Reference range: insoluble <−10 < poorly <−6 < moderately <−4 < soluble <−2 < very < 0 < highly.

3.2.4. Pharmacokinetics.

Pharmacokinetics (PK) plays a crucial role in determining the safety and efficacy of a therapeutic molecule. The PK describes the response of the biological system when drug molecules pass through it in terms of ADME. The absorption (A) distribution (D) features of selected ligands and inhibitors have been discussed in the previous section of the BOILED-Egg model of ADME. Biotransformation of therapeutic molecules through phase I metabolizing enzymes, especially cytochrome P450 isozymes (CYP450s), is an essential aspect of their metabolism (M) and excretion (E). SwissADME predicts whether a drug molecule is a substrate or inhibitor of five major CYP450s, viz., CYP1A2, CYP2C19, CYP2C9, CYP2D6, and CYP3A4. Inhibiting these CYP450 isozymes causes toxicity and undesirable effects due to the lower excretion and accrual of ingested drug molecules. The propensity of ligand hits towards the skin permeation (logKp) was predicted and found comparable to the selected inhibitors. The more negative the logKp value lower the skin permeation [38]. The details of predicted CYP450s metabolism and skin permeation of terpenoids and reference drugs are shown in Table 4.

Table 4. Computed pharmacokinetics of selected terpenoids and reference molecules.

Ligands	**CYP1A2**	**CYP2C19**	**CYP2C9**	**CYP2D6**	**CYP3A4**	**LogKp (cm/s)**
	Inhibitor					
Carnosol	No	No	Yes	No	No	-5.21
Jatropholone	Yes	Yes	Yes	No	Yes	-4.92
Rosmanol	No	No	No	Yes	No	-5.99
Tagitinin	No	No	No	No	No	-7.21
Ailanquassin	No	No	No	No	No	-8.44
Bigelovin	No	No	No	No	No	-7.31
Asiatic acid	No	No	No	No	No	-5.23
Aucubin	No	No	No	No	No	-10.56
6-alpha-hydroxyneopulchellin	No	No	No	No	No	-7.51
Sitagliptin	No	No	No	No	No	-8.29

3.2.5. Drug-likeness.

SwissADME tool implements five different pharmaceutical and biotechnology-based descriptors with varied arrays of screens that qualitatively estimate the affinity for a molecule to become a putative oral drug candidate vis-à-vis bioavailability. Abbott bioavailability score (BS) is a determinant of the oral absorption of a drug molecule. Although, similar physical properties do not apply to cations, anions, and uncharged molecules at physiologic pH, delineating their bioavailability and permeability. PSA for anions and RO5 for both cations and uncharged molecules has pretty enough forecasting ability. Abbot BS is 0.11 for anions showing PSA >150 Å2, 0.56 if PSA ranges 75-150 Å2, and 0.85 if PSA is less than 75 Å2. Abbot BS is 0.55 and 0.17, respectively, for the remaining compounds that comply and breach RO5. All virtually screened ligands and reference inhibitors exhibit an Abbott BS value of 0.55 means they fulfilled the criteria of oral drug molecules [39]. Details of computed drug-likeness of selected terpenoids and reference drugs are shown in Table 5.

Table 5. Computed drug-likeness of selected terpenoids and reference molecules.

Ligands	Lipinski	Ghose	Veber	Egan	Muegge	Bioavailability Score
	Violations					
Carnosol	0	0	0	0	0	0.55
Jatropholone	0	0	0	0	0	0.55
Rosmanol	0	0	0	0	0	0.55
Tagitinin	0	0	0	0	0	0.55
Ailanquassin	0	0	0	0	0	0.55
Bigelovin	0	0	0	0	0	0.55
Asiatic acid	0	3	0	0	1	0.56
Aucubin	1	1	1	1	2	0.55
6-alpha-hydroxyneopulchellin	0	0	0	0	0	0.55
Sitagliptin	0	0	0	0	0	0.55

3.2.6. Medicinal chemistry descriptors evaluation.

In medicinal chemistry attributes evaluation, respectively, Carnosol and Rosmanol were depicted as frequent hitters, i.e., Pan Assay Interference Structure (PAINS) alert, while other ligands were passed on PAINS parameter. Except for Jatropholone, all ligands and known drug sitagliptin exhibited undesirable moieties, i.e., Brenk alert. Moreover, Rosmanol, Bigelovin, Aucubin, and 6-alpha-hydroxyneopulchellin succeeded in lead-likeness features, while the remaining exhibited lead-likeness violations [40-42].

Synthetic accessibility (SA) is essential for the chemical synthesis of virtual molecules. The one and ten SA values represent very easy and challenging synthesis modes [43]. All molecules, including reference inhibitors, depicted an accessible synthesis mode reflected by their SA values (range: 3.5- 6.56). Computed medicinal chemistry attributes of selected terpenoids and reference molecules are shown in Table 6.

Table 6. Computed medicinal chemistry descriptors of selected terpenoids and reference molecules.

Ligands	PAINS alerts	Brenk alerts	Lead-likeness	SA
Carnosol	1	1	1	4.88
Jatropholone	0	0	1	3.86
Rosmanol	1	1	0	5.07
Tagitinin	0	4	1	5.61
Ailanquassin	0	1	1	5.77
Bigelovin	0	2	0	4.79
Asiatic acid	0	1	2	6.56
Aucubin	0	1	0	5.79
6-alpha-hydroxyneopulchellin	0	1	0	4.54
Sitagliptin	0	1	1	3.5

3.3. Molecular dynamics simulation.

Molecular dynamics (MD) simulation and normal mode analysis (NMA) of Asiatic acid and DPP IV docked complex was conducted to investigate amino acid residues' mobilities and flexibilities upon binding.

3.3.1. Mobility.

The main-chain (protein backbone) deformability is a determinant of the competence of a given molecule to distort at each of its residues. The position of the chain pivots can be inferred from high deformability areas. The deformability of the target protein upon binding with Asiatic acid is shown in Figure 7.

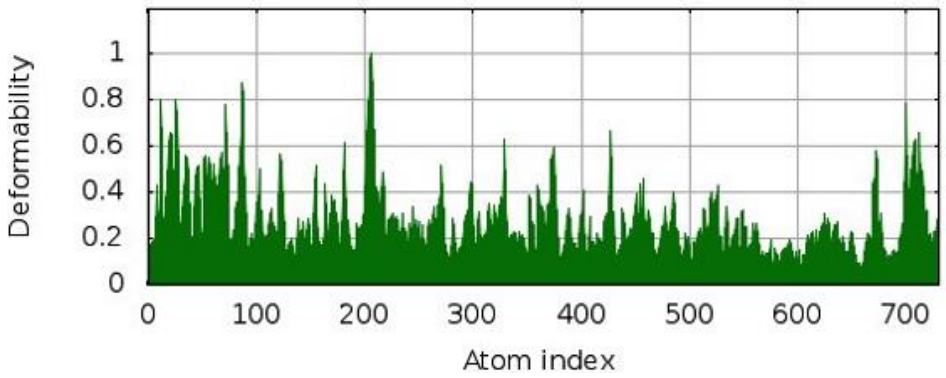

Figure 7. Deformability of DPP IV upon binding with Asiatic acid.

3.3.2. B-factor.

The experimental B-factor is taken from the corresponding PDB field, and the calculated from NMA is obtained by multiplying the NMA mobility by (8pi2). The B-factor column gives an averaged root mean square deviation (RMSD). The B-factor of DPP IV and Asiatic acid docked complex is shown in Figure 8.

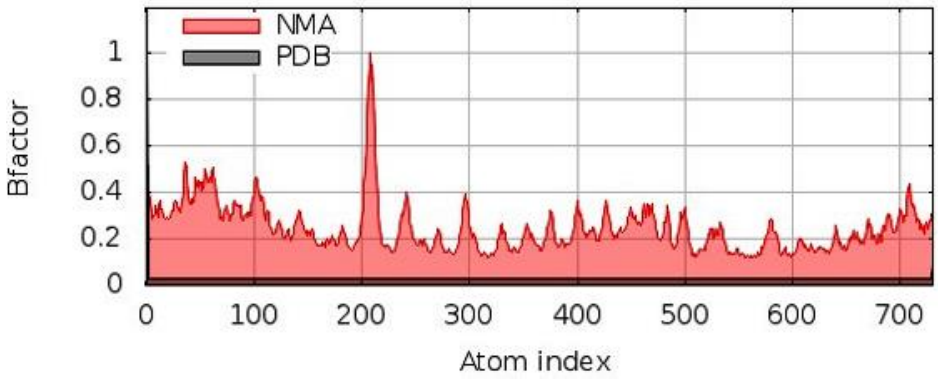

Figure 8. B-factor of DPP IV upon binding with Asiatic acid.

3.3.3. Eigenvalues.

The eigenvalue linked to each normal mode signifies the motion toughness. The eigenvalue is directly proportional to the energy needed to distort the structure. The lesser the eigenvalue, the easier the distortion (Figure 9).

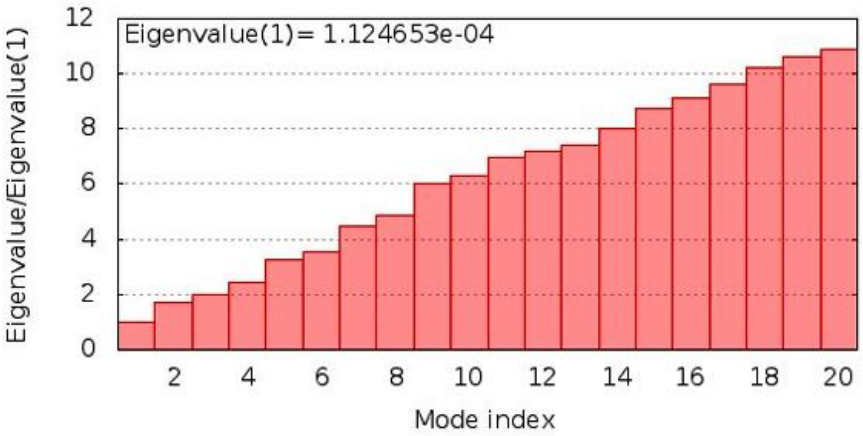

Figure 9. Eigenvalues of the docked complex of DPP IV and Asiatic acid.

3.3.4. Variance.

The variance related to each normal mode is inversely proportional to the eigenvalue. Colored bars display the individual (red) and cumulative (green) variances (Figure 10).

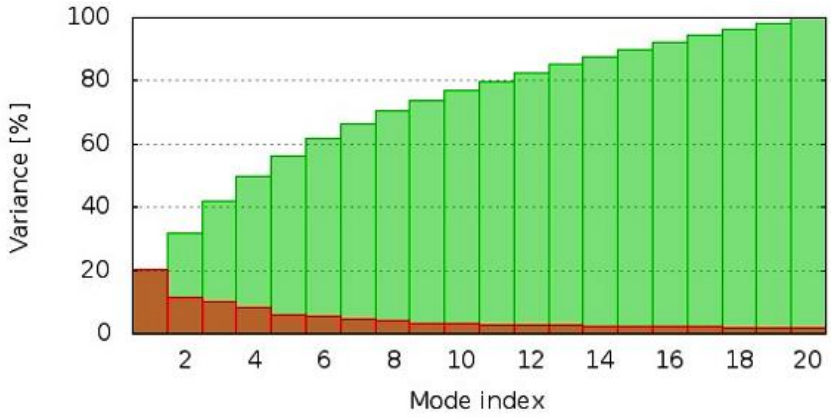

Figure 10. Variance of the docked complex of DPP IV and Asiatic acid. Variance. Red and green, respectively, show individual and cumulative variances.

3.3.5. Covariance map.

The covariance matrix designates coupling between pairs of residues, i.e., whether they experience correlated (red), uncorrelated (white), or anti-correlated (blue) motions (Figure 11) [44].

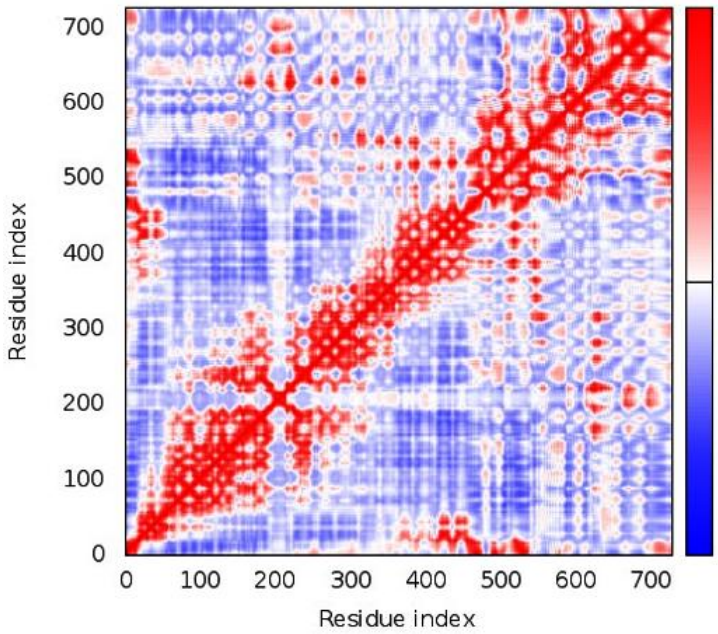

Figure 11. Covariance map of the docked complex of DPP IV and Asiatic acid. Variance. Red, white and blue, respectively, show correlated, uncorrelated, and anti-correlated motions.

3.3.6. Elastic network.

The elastic network model describes which pairs of atoms are linked by springs (Figure 12).

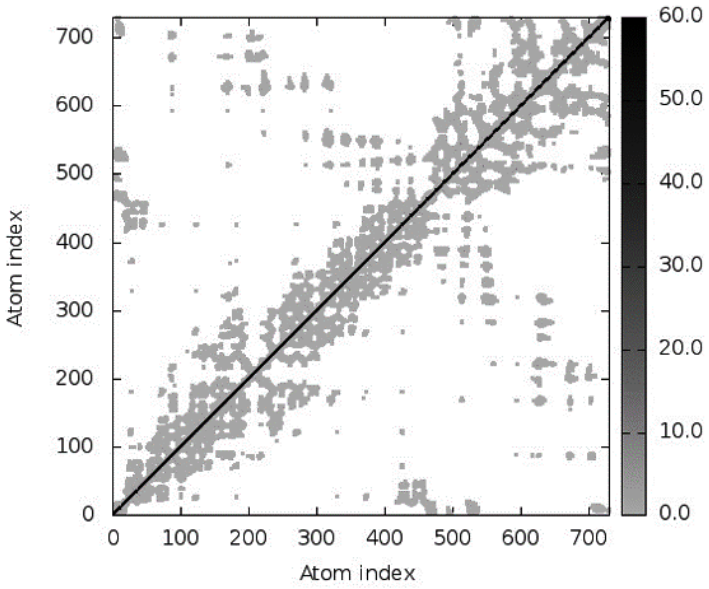

Figure 12. Elastic network: Each dot in the graph represents one spring between the corresponding pair of atoms. Dots are colored according to their toughness. Darker grey regions indicate compact regions.

4. Conclusions

Diabetes is one of the most pervasive disorders that cause millions of deaths across the globe every year, and it is independent of countries socioeconomic background. The constancy of diabetes for a long time directs to irreparable damage to vital organs. The persistence of diabetes may induce different microvascular and macrovascular intricacies, viz., Monckeberg arteriosclerosis, peripheral artery disease, coronary heart disease, cerebrovascular disease, peripheral neuropathy, erectile and bladder dysfunction, nephropathy, gastroparesis, retinopathy. Albeit multiple prophylactic and therapeutic medications are available, finding total control and cures for diabetes is still elusive. Thus, we must impede molecular targets accountable for high blood sugar levels via plant-derived phyto-ingredients in our dietary meals. In this context, DPP IV was selected as a therapeutic target. Identifying potential DPP IV inhibitors comparable to its known drug, molecular interaction studies with 513 terpenoids were carried out using ADT followed by MD simulation. Based on the ΔG, nine ligand hits were found as the top hits comparable to the reference drug Sitagliptin. Physicochemical properties, lipophilicity, solubility, drug-likeness, pharmacokinetics, medicinal chemistry features, molecular docking, and MD simulation analyses depicted Asiatic-DPP IV docked complex as more stable than the reference drug (Sitagliptin) complex. Based on the research findings, it is suggested that Asiatic acid exhibits excellent features of oral drugs. However, to validate the research finding, a holistic approach to wet-lab experiments is required before the manifestation of its therapeutic use.

Funding

This research received no external funding.

Acknowledgments

The authors would like to acknowledge Biotechnology Research Trust Fund.

Conflicts of Interest

The authors declare no conflict of interest.

References

1. Sun, H.; Saeedi, P.; Karuranga, S.; Pinkepank, M.; Ogurtsova, K.; Duncan, B. B.; Stein, C.; Basit, A.; Chan, J. C. N.; Mbanya, J. C.; Pavkov, M. E.; Ramachandaran, A.; Wild, S. H.; James, S.; Herman, W. H.; Zhang, P.; Bommer, C.; Kuo, S.; Boyko, E. J.; Magliano, D. J. IDF Diabetes Atlas: Global, Regional and Country-Level Diabetes Prevalence Estimates for 2021 and Projections for 2045. *Diabetes Res. Clin. Pract.* **2022**, *183*, 109119. https://doi.org/10.1016/j.diabres.2021.109119.
2. Ogurtsova, K.; Guariguata, L.; Barengo, N. C.; Ruiz, P. L.-D.; Sacre, J. W.; Karuranga, S.; Sun, H.; Boyko, E. J.; Magliano, D. J. IDF Diabetes Atlas: Global Estimates of Undiagnosed Diabetes in Adults for 2021. *Diabetes Res. Clin. Pract.* **2022**, *183*, 109118. https://doi.org/10.1016/j.diabres.2021.109118.
3. Wu, H.; Patterson, C. C.; Zhang, X.; Ghani, R. B. A.; Magliano, D. J.; Boyko, E. J.; Ogle, G. D.; Luk, A. O. Y. Worldwide Estimates of Incidence of Type 2 Diabetes in Children and Adolescents in 2021. *Diabetes Res. Clin. Pract.* **2022**, *185*, 109785. https://doi.org/10.1016/j.diabres.2022.109785.
4. Tönnies, T.; Rathmann, W.; Hoyer, A.; Brinks, R.; Kuss, O. Quantifying the Underestimation of Projected Global Diabetes Prevalence by the International Diabetes Federation (IDF) Diabetes Atlas. *BMJ Open Diabetes Res. Care* **2021**, *9* (1), e002122. https://doi.org/10.1136/bmjdrc-2021-002122.
5. Arneth, B.; Arneth, R.; Shams, M. Metabolomics of Type 1 and Type 2 Diabetes. *Int. J. Mol. Sci.* **2019**, *20*, 2467, https://doi.org/10.3390/ijms20102467.
6. Khan, M.A.B.; Hashim, M.J.; King, J.K.; Govender, R.D.; Mustafa, H.; Al Kaabi, J. Epidemiology of Type 2 Diabetes – Global Burden of Disease and Forecasted Trends. *J. Epidemiol. Glob. Health* **2020**, *10*, 107-111, https://doi.org/10.2991/jegh.k.191028.001.
7. Ahlqvist, E.; Prasad, R.B.; Groop, L. 100 YEARS OF INSULIN: Towards Improved Precision and a New Classification of Diabetes Mellitus. *J. Endocrinol.* **2021**, *252*, R59–R70, https://doi.org/10.1530/JOE-20-0596.
8. Yaping, X.; Chunhong, L.; Huifen, Z.; Fengfeng, H.; Huibin, H.; Meijing, Z. Risk Factors Associated with Gestational Diabetes Mellitus: A Retrospective Case-Control Study. *Int. J. Diabetes Dev. Ctries.* **2022**, *42*, 91–100, https://doi.org/10.1007/s13410-021-00947-3.
9. Yamamoto, J.M.; Donovan, L.E.; Mohammad, K.; Wood, S.L. Severe Neonatal Hypoglycaemia and Intrapartum Glycaemic Control in Pregnancies Complicated by Type 1, Type 2 and Gestational Diabetes. *Diabet. Med.* **2020**, *37*, 138–146, https://doi.org/10.1111/dme.14137.
10. Saeedi, P.; Petersohn, I.; Salpea, P.; Malanda, B.; Karuranga, S.; Unwin, N.; Colagiuri, S.; Guariguata, L.; Motala, A.A.; Ogurtsova, K.; Shaw, J.E.; Bright, D.; Williams, R. Global and Regional Diabetes Prevalence Estimates for 2019 and Projections for 2030 and 2045: Results from the International Diabetes Federation Diabetes Atlas, 9th Edition. *Diabetes Res. Clin. Pract.* **2019**, *157*, 107843, https://doi.org/10.1016/j.diabres.2019.107843.
11. Kausar, M.A.; Shahid, S.; Anwar, S.; Kuddus, M.; Khan, M.K.A.; Alotaibi, A.D.; Arif, J.M. Identifying Natural Therapeutics against Diabetes via Inhibition of Dipeptidyl Peptidase 4: Molecular Docking and MD Simulation Study. *Indian J. Pharm. Educ. Res.* **2022**, *56*, s21–s31, https://doi.org/10.5530/ijper.56.1s.39.
12. Prasad, V.; Mailankody, S. Assessing Pharmaceutical Research and Development Costs—Reply. *JAMA Intern. Med.* **2018**, *178*, 588-589, https://doi.org/10.1001/jamainternmed.2017.8737.
13. Jensterle, M.; Janez, A.; Fliers, E.; DeVries, J.H.; Vrtacnik-Bokal, E.; Siegelaar, S.E. The Role of Glucagon-like Peptide-1 in Reproduction: From Physiology to Therapeutic Perspective. *Hum. Reprod. Update* **2019**, *25*, 504–517, https://doi.org/10.1093/humupd/dmz019.
14. Chia, C.W.; Egan, J.M. Incretins in Obesity and Diabetes. *Ann. N. Y. Acad. Sci.* **2020**, *1461*, 104–126, https://doi.org/10.1111/nyas.14211.
15. Holst, J.J. The Incretin System in Healthy Humans: The Role of GIP and GLP-1. *Metabolism* **2019**, *96*, 46–55, https://doi.org/10.1016/j.metabol.2019.04.014.
16. Marathe, C.S.; Pham, H.; Marathe, J.A.; Trahair, L.G.; Huynh, L.; Wu, T.; Phillips, L.K.; Rayner, C. K.; Nauck, M.A.; Horowitz, M.; Jones, K.L. The Relationship between Plasma GIP and GLP-1 Levels in Individuals with Normal and Impaired Glucose Tolerance. *Acta Diabetol.* **2020**, *57*, 583–587, https://doi.org/10.1007/s00592-019-01461-z.

17. Hassanabad, M.F.; Hassanabad, A.F.; Fatehi, M. Do Dipeptidyl Peptidase-4 Inhibitors Increase the Risk of Heart Failure in Patients with Type 2 Diabetes? *Curr. Diabetes Rev.* **2022**, *18*, e161221199093, https://doi.org/10.2174/1573399818666211216144900.
18. de Bhailís, Á.M.; Azmi, S.; Kalra, P.A. Diabetic Kidney Disease: Update on Clinical Management and Non-Glycaemic Effects of Newer Medications for Type 2 Diabetes. *Ther. Adv. Endocrinol. Metab.* **2021**, *12*, 204201882110206, https://doi.org/10.1177/20420188211020664.
19. Zheng, W.; Zhou, J.; Song, S.; Kong, W.; Xia, W.; Chen, L.; Zeng, T. Dipeptidyl-Peptidase 4 Inhibitor Sitagliptin Ameliorates Hepatic Insulin Resistance by Modulating Inflammation and Autophagy in Ob/Ob Mice. *Int. J. Endocrinol.* **2018**, *2018*, 8309723, https://doi.org/10.1155/2018/8309723.
20. Morris, G.M.; Goodsell, D.S.; Halliday, R.S.; Huey, R.; Hart, W.E.; Belew, R.K.; Olson, A.J. Automated Docking Using a Lamarckian Genetic Algorithm and an Empirical Binding Free Energy Function. *J. Comput. Chem.* **1998**, *19*, 1639–1662, https://doi.org/10.1002/(SICI)1096-987X(19981115)19:14<1639::AID-JCC10>3.0.CO;2-B.
21. Furuhashi, M.; Sakuma, I.; Morimoto, T.; Higashiura, Y.; Sakai, A.; Matsumoto, M.; Sakuma, M.; Shimabukuro, M.; Nomiyama, T.; Arasaki, O.; Node, K.; Ueda, S. Differential Effects of DPP-4 Inhibitors, Anagliptin and Sitagliptin, on PCSK9 Levels in Patients with Type 2 Diabetes Mellitus Who Are Receiving Statin Therapy. *J. Atheroscler. Thromb.* **2022**, *29*, 24-37, https://doi.org/10.5551/jat.58396.
22. Morris, G.M.; Goodsell, D.S.; Huey, R.; Olson, A.J. Distributed Automated Docking of Flexible Ligands to Proteins: Parallel Applications of AutoDock 2.4. *J. Comput. Aided. Mol. Des.* **1996**, *10*, 293–304, https://doi.org/10.1007/BF00124499.
23. Khan, F.I.; Lai, D.; Anwer, R.; Azim, I.; Khan, M.K.A. Identifying Novel Sphingosine Kinase 1 Inhibitors as Therapeutics against Breast Cancer. *J. Enzyme Inhib. Med. Chem.* **2020**, *35*, 172–186, https://doi.org/10.1080/14756366.2019.1692828.
24. Khan, M.K.A.; Ahmad, S.; Rabbani, G.; Shahab, U.; Khan, M.S. Target-based Virtual Screening, Computational Multiscoring Docking and Molecular Dynamics Simulation of Small Molecules as Promising Drug Candidate Affecting Kinesin-like Protein KIFC1. *Cell Biochem. Funct.* **2022**, *40*, 451–472, https://doi.org/10.1002/cbf.3707.
25. Sharma, A.; Singh, K.; Upadhyay, T.K.; Hayat-ul-Islam, M.; Khan, M.K.A.; Dwivedi, U.N.; Sharma, R. Structure-Based *In silico* and *In vitro* Analysis Reveals Asiatic Acid As Novel Potential Inhibitor of *Mycobacterium Tuberculosis* Maltosyl Transferase. *Curr. Comput. Aided. Drug Des.* **2022**, *18*, 213-227, https://doi.org/10.2174/1573409918666220623105908.
26. Khan, M.K.A.; Akhtar, S.; Arif, J.M. Development of *In silico* Protocols to Predict Structural Insights into the Metabolic Activation Pathways of Xenobiotics. *Interdiscip. Sci. Comput. Life Sci.* **2018**, *10*, 329–345, https://doi.org/10.1007/s12539-017-0237-4.
27. Ahmad Khan, M.K.; Akhtar, S.; Al-Khodairy, F. Molecular Docking Approach to Elucidate Metabolic Detoxification Pathway of Polycyclic Aromatic Hydrocarbons. *NeuroPharmac J.* **2021**, *6*, 150–161, https://doi.org/10.37881/1.613.
28. Khan, M.K.A.; Akhtar, S.; Arif, J.M. Structural Insight into the Mechanism of Dibenzo[a,l]Pyrene and Benzo[a]Pyrene-Mediated Cell Proliferation Using Molecular Docking Simulations. *Interdiscip. Sci. Comput. Life Sci.* **2018**, *10*, 653–673, https://doi.org/10.1007/s12539-017-0226-7.
29. Kausar, M.A.; Shahid, S.; Anwar, S.; Kuddus, M.; Khan, M.K.A.; Khalifa, A.M.; Khatoon, F.; Alotaibi, A.D.; Alkhodairy, S.F.; Snoussi, M.; Arif, J.M. Identifying the Alpha-Glucosidase Inhibitory Potential of Dietary Phytochemicals against Diabetes Mellitus Type 2 via Molecular Interactions and Dynamics Simulation. *Cell. Mol. Biol.* **2022**, *67*, 16–26, https://doi.org/10.14715/cmb/2021.67.5.3.
30. Daina, A.; Michielin, O.; Zoete, V. SwissADME: A Free Web Tool to Evaluate Pharmacokinetics, Drug-Likeness and Medicinal Chemistry Friendliness of Small Molecules. *Sci. Rep.* **2017**, *7*, 42717, https://doi.org/10.1038/srep42717.
31. Lopéz-Blanco, J.R.; Garzón, J.I.; Chacón, P. IMod: Multipurpose Normal Mode Analysis in Internal Coordinates. *Bioinformatics* **2011**, *27*, 2843–2850, https://doi.org/10.1093/bioinformatics/btr497.
32. Attique, S.; Hassan, M.; Usman, M.; Atif, R.; Mahboob, S.; Al-Ghanim, K.; Bilal, M.; Nawaz, M.Z. A Molecular Docking Approach to Evaluate the Pharmacological Properties of Natural and Synthetic Treatment Candidates for Use against Hypertension. *Int. J. Environ. Res. Public Health* **2019**, *16*, 923, https://doi.org/10.3390/ijerph16060923.
33. Egan, W.J.; Merz, K.M.; Baldwin, J.J. Prediction of Drug Absorption Using Multivariate Statistics. *J. Med. Chem.* **2000**, *43*, 3867–3877, https://doi.org/10.1021/jm000292e.

34. Egan, W.J.; Lauri, G. Prediction of Intestinal Permeability. *Adv. Drug Deliv. Rev.* **2002**, *54*, 273–289, https://doi.org/10.1016/S0169-409X(02)00004-2.
35. O'Boyle, N.M.; Banck, M.; James, C.A.; Morley, C.; Vandermeersch, T.; Hutchison, G.R. Open Babel: An Open Chemical Toolbox. *J. Cheminform.* **2011**, *3*, 33, https://doi.org/10.1186/1758-2946-3-33.
36. Ertl, P.; Rohde, B.; Selzer, P. Fast Calculation of Molecular Polar Surface Area as a Sum of Fragment-Based Contributions and Its Application to the Prediction of Drug Transport Properties. *J. Med. Chem.* **2000**, *43*, 3714–3717, https://doi.org/10.1021/jm000942e.
37. Ali, J.; Camilleri, P.; Brown, M.B.; Hutt, A.J.; Kirton, S.B. Revisiting the General Solubility Equation: *In silico* Prediction of Aqueous Solubility Incorporating the Effect of Topographical Polar Surface Area. *J. Chem. Inf. Model.* **2012**, *52*, 420–428, https://doi.org/10.1021/ci200387c.
38. Potts, R.O.; Guy, R.H. Predicting Skin Permeability. *Pharm. Res. An Off. J. Am. Assoc. Pharm. Sci.* **1992**, *9*, 663–669, https://doi.org/10.1023/A:1015810312465.
39. Martin, Y.C. A Bioavailability Score. *J. Med. Chem.* **2005**, *48*, 3164–3170, https://doi.org/10.1021/jm0492002.
40. Baell, J.B.; Holloway, G.A. New Substructure Filters for Removal of Pan Assay Interference Compounds (PAINS) from Screening Libraries and for Their Exclusion in Bioassays. *J. Med. Chem.* **2010**, *53*, 2719–2740, https://doi.org/10.1021/jm901137j.
41. Brenk, R.; Schipani, A.; James, D.; Krasowski, A.; Gilbert, I.H.; Frearson, J.; Wyatt, P.G. Lessons Learnt from Assembling Screening Libraries for Drug Discovery for Neglected Diseases. *ChemMedChem* **2008**, *3*, 435–444, https://doi.org/10.1002/cmdc.200700139.
42. Teague, S.J.; Davis, A.M.; Leeson, P.D.; Oprea, T. The Design of Leadlike Combinatorial Libraries. *Angew. Chemie Int. Ed.* **1999**, *38*, 3743–3748, https://doi.org/10.1002/(SICI)1521-3773(19991216)38:24<3743::AID-ANIE3743>3.0.CO;2-U.
43. Ertl, P.; Schuffenhauer, A. Estimation of Synthetic Accessibility Score of Drug-like Molecules Based on Molecular Complexity and Fragment Contributions. *J. Cheminform.* **2009**, *1*, 8, https://doi.org/10.1186/1758-2946-1-8.
44. Ichiye, T.; Karplus, M. Collective Motions in Proteins: A Covariance Analysis of Atomic Fluctuations in Molecular Dynamics and Normal Mode Simulations. *Proteins Struct. Funct. Bioinf.* **1991**, *11*, 205–217, https://doi.org/10.1002/prot.340110305.